

CHART Scientific Report 2023

FCC-ee Injector Study and the P³ Project at PSI

P. Craievich, S. Bettoni, M. Schär, N. Vallis, R. Zennaro, B. Auchmann, H. H. Braun,
M. I. Besana, M. Duda, R. Fortunati, H. Garcia-Rodrigues, D. Hauenstein, R.
Ischebeck, E. Ismaili, P. Juranić, J. Kosse, F. Marcellini, T. Michlmayr, S. Müller, M.
Pedrozzi, R. Rotundo, G. L. Orlandi, M. Seidel, N. Strohmaier, M. Zykova
PSI, Villigen, Switzerland

A. Grudiev, A. Latina, S. Doebert, Z. Vostrel, Y. Zhao, B. Humann, A. Lechner, A.
Kurtulus, R. Mena Andrade, J.-L. Grenard, A. Perillo-Marccone, M. Calviani, W.
Bartmann, Y. Duthell, H. Bartosik, K. Oide, F. Zimmermann, M. Benedikt
CERN, Geneva, Switzerland

I. Chaikovska, F. Alharthi, V. Mytrochenko, R. Chehab, *CNRS/IJCLab, Orsay, France*

C. Milardi, A. De Santis, O. Etisken, S. Spampinati, *LNF/INFN, Frascati, Italy*

T. Rauberheimen, *SLAC, Menlo Park, CA, United States*

Y. Enomoto, *KEK, Tsukuba, Japan*

January 2024

This report provides an insight into the progress of the FCC-ee Injector Study collaboration in the framework of the CHART proposal over the past 12 months. The report is organised with a section for each work package to highlight the results achieved for each topic.

Contents

1 Overall Parameter Optimization (WP0)	2
1.1 Pre-injector layout with a damping ring at higher beam energy	5
2 Electron Source, Electron and Positron Linacs (WP1, WP2)	5
2.1 Electron Source	5

2.2 Electron and Positron Linacs	7
3 Positron Source: Target and Capture System (WP3)	10
4 Damping Ring and Transfer Lines (WP4)	13
5 PSI Positron Production (P³) Project (WP6)	18
References	21
Publications and Conference Contributions	24

1 Overall Parameter Optimization (WP0)

The FCC-ee pre-injector complex must provide the electron and positron bunch trains for alternating bootstrapping injection during both top-up and filling from scratch operations. The most demanding collider operation mode in terms of bunch population in the single bucket is the Z-pole running [1]. Considering the charge per bucket and lifetime for this operational mode then an alternating injection of a train of positrons and electrons approximately every few tens of seconds is required to ensure the correct balance within 5% between positron and electron bunch charges during collider operation. The baseline described in the CDR [1] considers a 6 GeV linac, with two bunches per RF pulse with a time separation between 15 ns and 25 ns, with a repetition rate up to 200 Hz and two possible options for the pre-injector complex. In the first option, the 6 GeV bunches are injected into the existing Super Proton Synchrotron (SPS) ring, while in the second option, an additional High-Energy (HE) linac would increase the energy from 6 GeV to 20 GeV and inject the beams directly into the Booster Ring (BR). Table 1 lists the specifications to be considered as target parameters at the pre-injector end for the two options. It is worth noting that the maximum charge to be injected into the collider rings at each injection from the booster is about 4 nC (bunch population $2.5 \cdot 10^{10}$ particles), and considering a transmission efficiency between the different accelerators, such as between the linac and the booster ring (BR) and the BR and the collider rings (CRs), of 80%, then the pre-injector must guarantee a charge of about 5 nC at the end of the pre-injector.

Figure 1 schematically shows the latest basic layout of the pre-injector complex. It includes two separate linacs for electrons and positrons up to a beam energy of 1.54 GeV – the Electron Linac (e-Linac) and the Positron Linac (p-Linac), respectively. For the positron production mode, following the e-Linac, the electron bunches will share a second linac, the Common Linac, with the positron bunches coming from the damping ring. The common Linac (c-Linac) will increase the energy of both species to an energy of 6 GeV. The schematic layout also includes the high-energy (HE) linac, which boosts the beam energy from 6 GeV up to 20 GeV in order to inject beams directly into the BR without passing through the Super Proton Synchrotron (SPS) ring. The baseline for the positron source is based on a conventional scheme using electrons from the common

Table 1: Target parameters for latest baseline layout of the pre-injector for the Z-pole in the collider.

	Baseline	HE Linac	Unit
Ring for injection	PBR	BR	
Injection energy	6	20	GeV
Single bunch charge	4	4	nC
Repetition rate	200	200	Hz
Number of bunches	2	2	
Bunch spacing	15 – 25	15 – 25	ns
Rms nor. emittance (x, y)	50, 50	10, 10	mm.mrad
Rms bunch length	≈ 1	≈ 1	mm
Rms energy spread	0.3	≈ 0.1	%

linac at 6 GeV impinging on a tungsten target while two options are currently being considered for the Adiabatic Matching Device (AMD). The first involves the use of a Flux Concentrator (FC), which makes use of a pulsed magnet, a technology currently used in the SuperKEKB collider positron source, while the second involves the use of a superconducting solenoid (SC). The technology used to make the solenoid is based on High-Temperature Superconducting (HTS) tape, and a demonstrator will be tested in the SwissFEL linac at PSI. Following the positron linac, an energy compressor system is used to reduce the incoming beam energy spread in order to maximize the injection efficiency into the Damping Ring (DR) for emittance reduction. A complex and long transfer line system is used to bring back the positron beam from the DR to the common linac where it is accelerated up to 6 GeV. The transfer lines system includes doglegs to implement injection and extraction in and from the DR, and arcs to bring back the low-emittance positron beam to the entrance of the common linac stage. A bunch compressor is also used to keep under control the bunch length of the positron beam before the injection in the common linac.

During the process of generating positrons, both positron and electron bunches must be accelerated in the common linac. There are two possible configurations being considered for the temporal structure. In the first configuration, positron and electron bunches are accelerated in separate RF pulses that are spaced 2.5 ms apart, resulting in an effective repetition rate of 400 Hz (2×200 Hz). This arrangement poses challenges for the RF source, the klystron, and the accelerating structures, as they all need to work at such a high repetition rate and handle the associated high power dissipation. Alternatively, in the second configuration, two bunches of positrons and two bunches of electrons are accelerated within the same RF pulse with a repetition rate of 200 Hz. Accommodating four bunches within a single RF pulse presents even more significant difficulties for the low-level RF system, and the feasibility of this approach must be thoroughly examined. Additionally, a more fundamental issue would be the requirement for different magnet settings for electron and positron bunches. The currently baseline is the configuration in which the common linac is operated at 400 Hz.

The top-up operation also still needs to be clarified in order to define the lower limit of

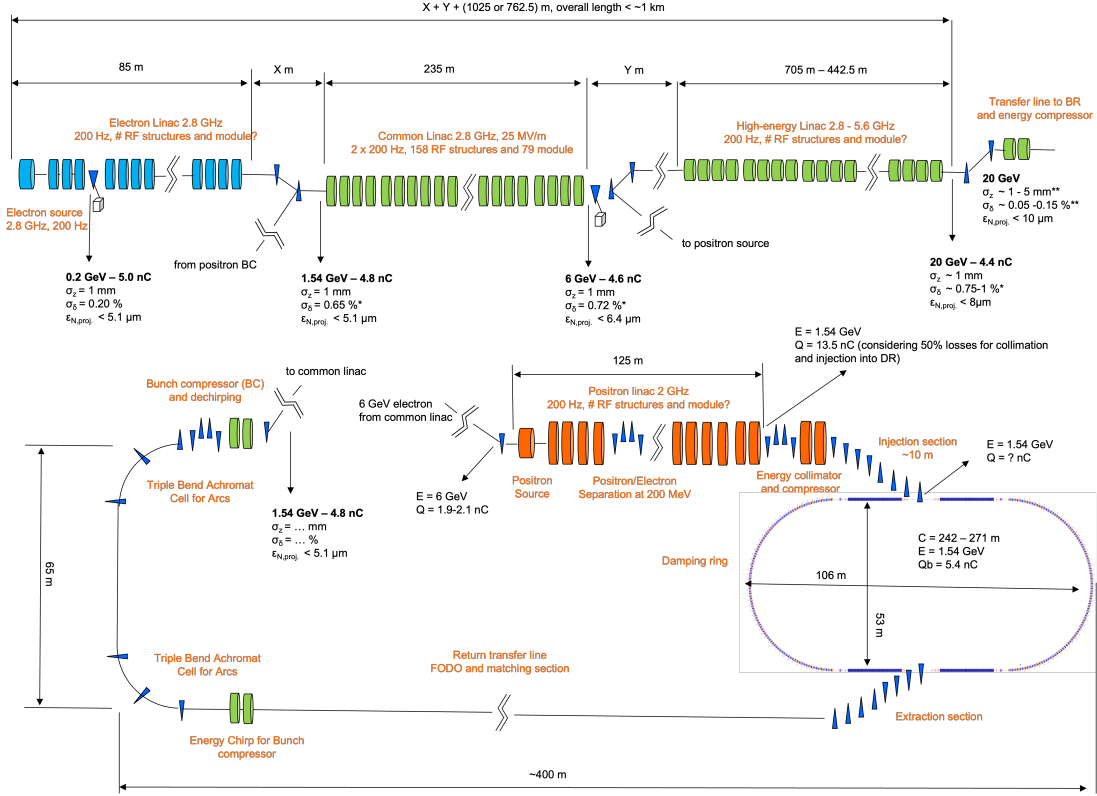


Figure 1: Latest baseline layout of the pre-injector complex including the high-energy (HE) linac.

the charge variation, which should arbitrarily vary from 0% to 100%. This requirement results from the different lifetimes of the individual bunches in the collider rings, which will also determine the filling pattern for each injection. Regarding to the emittance, the specification for the injection into the BR requires a rounded beam with an rms normalized emittance of 10 mm.mrad in both planes to ensure a shorter cycle in the booster itself. This specification has an impact on both electron source and DR parameters. In particular, the electron source must guarantee this emittance value even during the required charge variation for top-up operation, and this question has an impact on the optimization of the photo-cathode RF gun. Currently, the existing baseline does not include the use of the DR for electron bunch and this particular option will undergo a thorough review in the future.

In order to achieve independent design specifications for the linacs in the pre-injector from those of the BR, an energy compressor is planned in the transfer line from the HE linac to the BR. This arrangement is depicted in the top left part of the figure 1. By adopting this approach, the design of the linacs can converge towards a solution for the beam length and energy spread at the linac end specified in 1 without considering more complex layouts that include compression and/or decompression of the beam along the

different linacs.

The design process of pre-injector study is also collected in two scientific reports where the results are presented in more detail including a comprehensive list of references [11, 12].

1.1 Pre-injector layout with a damping ring at higher beam energy

As it will be seen in Tab. 7, in later chapters of the text, the current positron yield estimate allows for some consideration concerning the production of positrons at lower electron beam energy and higher-energy for the DR. A schematic layout considering a DR at 2.86 GeV is shown in Fig. 2.

This approach allows all linacs to operate at 200 Hz with 2-bunch to meet the CR filling

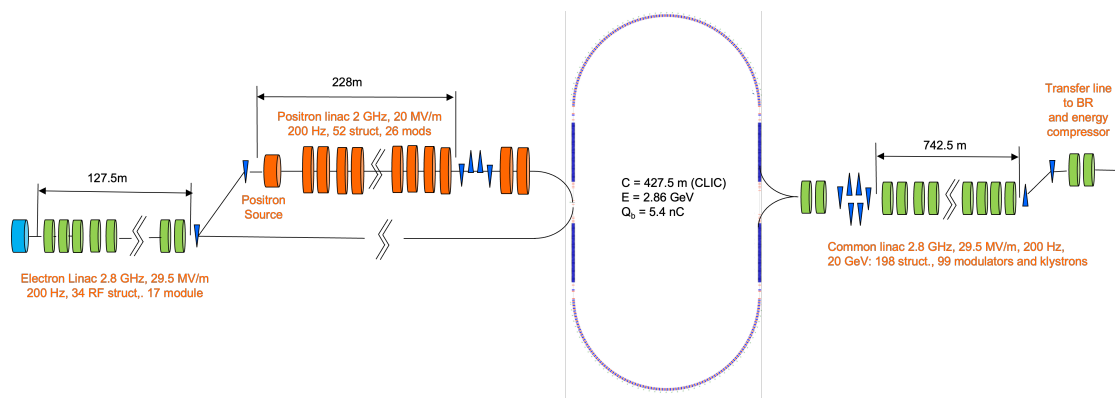


Figure 2: Schematic layout of the pre-injector with a damping ring at higher energy. linac. EC: Energy Compressor, BC: Bunch Compressor.

specification without having to provide for challenging 400 Hz operation of the common linac. A dedicated linac for electrons and positrons up to 2.86 GeV leads to considerable simplification in operations while maintaining or reducing the total acceleration length. For example, simpler operation of the common linac in terms of seconds instead of milliseconds between positron and electron operations. Furthermore, with this approach, no positron return line and arc are required.

2 Electron Source, Electron and Positron Linacs (WP1, WP2)

2.1 Electron Source

The most recent baseline configuration of the injector complex, as illustrated in Fig. 1, includes a single electron source for the production of both the nominal electron beam and the driver electron beam for positrons production. Extensive simulations has been conducted on the electron source, which involves employing an photo-cathode RF gun followed by acceleration to approximately 200 MeV. This particular configuration has

been thoroughly studied and is now established as the fundamental design for the pre-injector. The primary specification for the electron source is to generate a bunch with a charge of 5 nC while maintaining a normalized emittance below 10 mm.mrad, as per the requirements for injection into the main beam ring (BR).

Furthermore, investigations into the yield of positron production indicate that 5 nC electron bunches are sufficient to achieve the desired positron bunch charge. Various distribution models, such as uniform and truncated Gaussian, have been examined. The following beam parameters can be attained at the end of the electron source, specifically at 200 MeV, effectively meeting the specified requirements. These parameters, along with the simulated distributions, have been utilized as inputs for the subsequent design and simulations of the down-stream linacs. Please refer to Table 2 for the specific source parameters.

The latest baseline layout of the injector complex, as illustrated in Fig. 1, includes a single electron source for the production of both positrons and electrons. The electron source is composed from a photo-cathode 2.6 cell RF photo gun followed from three RF accelerating structures to reach the beam energy of approximately 200 MeV. The main specification for the electron source is to generate a bunch with a charge of 5 nC keeping the normalized emittance below 4 mm.mrad in order to have a margin in any emittance growth along the linacs and transfer lines between linacs. Both uniform and truncated Gaussian distributions have been studied and table lists the optimized beam parameters that were achieved at the end of the electron source. These parameters and the simulated distributions have been used as input for the design and simulations of the following linacs.

One of the most challenging aspects for the electron source is the top-up operation mode

Table 2: Electron Source beam parameters at 200 MeV with a bunch charge of 5 nC.

Parameter	Uniform Distribution	Gaussian Distribution
Transverse Emittance [mmrad]	2	3
Energy Spread rms[%]	0.4	0.25
Bunch Length rms (mm)	0.98	1.3

for the collider. In this operational mode, the bunches circulating in the collider rings will be topped up with charge according to the charge decreasing during a collision. Therefore the injector has to deliver varying bunch charges in the range of 10-100% for each bunch. Since we operate in a two bunch per rf pulse scheme with a distance of 15-25 ns it will be likely not possible to change the charge within these two pulses if the cathode is driven by only one laser. To enable this possibility, two independent lasers need to be foreseen. The source and the linac will work with a 200 Hz repetition rate, leaving 5 ms between pulses to adjust laser, RF or magnet parameters. A detailed beam dynamics study has been started to determine which parameters need to be changed for different bunch charges to deliver as similar beams as possible. The best option would be to leave RF and magnet parameters constant and change only the laser spot size on the cathode so that the charge density stays as similar as possible. The spot size could be

manipulated fast enough using a controllable mirror array. Simulations show that, in this case, the beam parameter variation at the exit of the electron source is not to big (see Fig. 3).

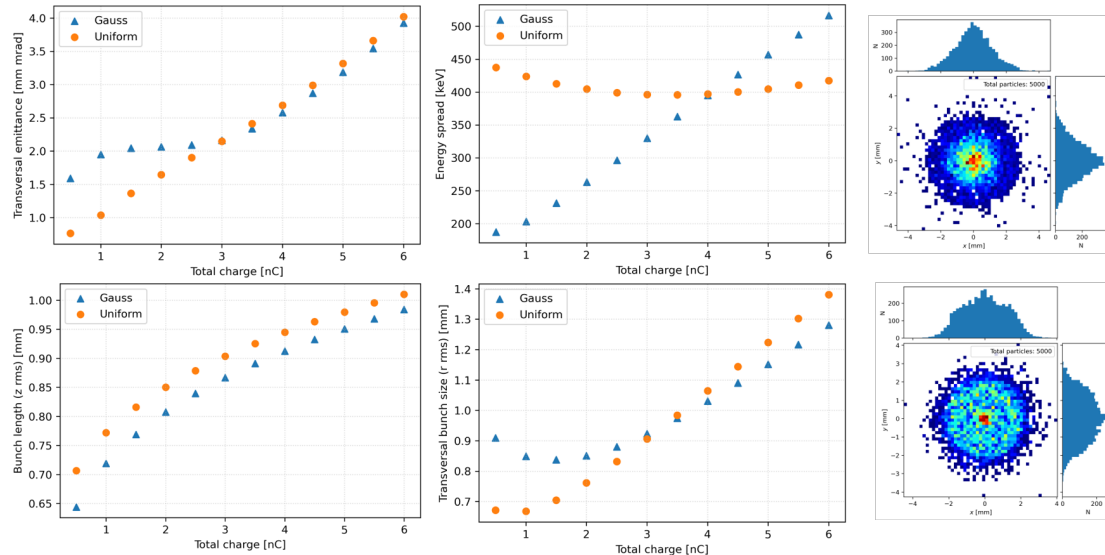


Figure 3: Beam parameter variation as a function of bunch charge simulating the top-up operation of the electron source and pre-injector.

2.2 Electron and Positron Linacs

Extensive beam dynamics simulations have been done to study both longitudinal and transverse beam dynamics. The main purpose was to define the design specifications for RF structures in terms of iris aperture, working frequency, structure length, gradient, etc.. In the context of longitudinal dynamics, the study considered two options: without and with an energy compressor to be installed in the transfer line between the pre-injector and the booster ring. The solution with the energy compressor leaves more room for variation of the beam parameters in order to meet the injection specifications in the BR. Fig. 1 shows the bunch length, relative energy spread and emittance at the end of the different linacs for the case of the 5 nC electron bunch. As can be seen, the specifications in Tab. 1 are met, and with the energy compressor it is possible to achieve a wide range of variations in bunch length and relative energy spread, see beam parameters listed on the top right in Fig. 1.

According to the simulation results collected in [11, 12], we are converging with the definition of the RF structures for the different linacs. The RF parameters of the accelerating structures for the linacs are collected in the Tab. 3. For the p-linac, 30+1 2-GHz three-meter-long type accelerating structures are required to reach a positron energy of 1.54 GeV. The module layout consists of one HV modulator, one klystron with a $5\text{-}\mu\text{s}$

RF pulse length, one pulse compressor and two three-meter long structures. Assuming power losses in the waveguide system and klystrons operating at 90% of their RF power specifications, the required number of modules is then 15+1. The klystrons peak RF power specification is 80 MW. For the e-Linac, the three-meter 2.8-GHz structure with an average aperture radius of 16.1 mm is very attractive because it has the high effective shunt impedance. An RF module consists of one HV modulator, one klystron, one pulse compressor and two three-meter long structures. To achieve an energy gain of 1.54 GeV in this configuration and assuming on-crest operation, 10+1 RF modules are required with a klystron RF peak power specification of 80 MW and an RF pulse width of 3 μ s. One of the salient features of the common linac is its operation at a 400 Hz repetition rate. In this case to keep under control the dissipated power in the RF system and using the same 2.8-GHz RF structure as in the e-linac then 70 RF structures are necessary to reach the beam energy of 6 GeV. With two RF structures, a klystron with a peak power of 50 MW and using an RF pulse compressor then 35 modules are necessary to reach the beam energy of 6 GeV.

For HE linac, the baseline remains the S-band operational frequency, although the C-band frequency could bring some benefit in terms of power consumption. Table 4 shows the estimated plug-power required for the linacs at the pre-injector. As can be seen, the network power for the HE linac with the C-band option is 30% lower compared to the S-band option. However, the S-band option has important advantages including the possibility of using the same RF module as in the e-linac, which uses most of the RF components of the c-linac. This aspect is very cost-effective in terms of spare parts and maintenance costs. It is also more suitable for beam dynamics because the iris aperture is larger and the RF curvature is smaller compared to the C-band option. Furthermore, the S-band technology is much more available on the market and also more mature, This last aspect when considered together with the costs which are similar to the C-band option has led to the conclusion that for linac HE the S-band option is the most cost-effective.

For the RF power sources i.e. klystrons, one of the technical challenges for the positron, electron and common linacs is the high repetition rates that are under consideration, 200 Hz for the positron and electron linacs and 400 Hz for the common linac. Moreover, there is no klystron designed to operate at 2 GHz. At 2.8 GHz, although there are no klystron at this specific frequency, many klystrons have demonstrated reliable performances at 2.856 GHz. Consequently, frequency adjustments on the klystron cavities would certainly reduce the development cost of such klystrons. The high average RF power resulting from higher repetition rates would be dealt with by redesigning the water cooling system of the klystron body and collector. Several companies have been contacted to assess the feasibility of klystrons operating at 2 GHz, 2.8 GHz and 5.6 GHz. One of these companies provided us with peak RF power levels that could be achieved at repetition rates of 200 Hz and 400 Hz for an RF pulse length of 3 μ s and 5 μ s - see Tab. 5.

To evaluate the impact of different charge values for the top-up operation, simulations were performed by varying the beam charge from 10% to 100%. The results showed that although charge variations affect the longitudinal dynamics of the beam, the current

Table 3: RF module summary table for all linacs. For RF power from the klystron, waveguide losses and 90% of the available RF power are taken into account. Two BPMs, two quadrupoles and two correctors are included in each RF module.

	p-linac	e-linac	c-linac	HE-linac S-band	HE-linac C-band	Unit
Frequency	2	2.8	2.8	2.8	5.6	GHz
Repetition rate	200	200	400	200	200	Hz
Min. iris radius	30	16.1	16.1	16.1	10.2	mm
Length	3	3	3	3	3	m
Filling time	447	486	486	1486	334	ns
SLED/BOC coupling	17	15	15	15	10	
RF pulse length	5	3	3	3	3	μ s
Average gradient	20	29.5	23.4	29.5	28.8	MV/m
Energy gain per structure	60	88.5	70.2	88.5	86.4	MeV
Klystron power per struct.	31	30	18.9	30	18.2	MW
Klystron max. power	80	80	50	80	50	MW
Structures per klystron	2	2	2	2	2	
Number of structures	1+30	1+20	70	164	172	
Number of rf modules	1+15	1+10	35	82	86	
Length of all modules	140	90	262.5	615	645	m

Table 4: Comparison of the plug-powers for the linacs at the pre-injector.

Linac	Plug-power [MW]	
klystron efficiency [%]	42	65
p-linac	6.1	4.0
e-linc	3.2	2.1
c-linac	12.5	8.3
Total p-, e-, c-linac	21.8	14.5
HE linac - S band option	23.6	16.0
HE linac - C band option	15.2	11.1

linac configuration allows for accommodating various levels of charge required for the top up operation. The different charge corresponds to different beam loading, which results in different energy and energy spread at the end of the common linac. The energy compressor between the linac end and the transfer line to the BR can still be used to compensate for these effects. The system converts the energy separation between the first and second bunch into time separation due to the non-zero R_{56} . In such a way, the bunches travel through downstream RF structures so that they experience different RF phases and finally different energy gains. In so doing, this system can be used to compensate for the difference in energy gain and energy spread from bunch to bunch due to the different beam intensity. This approach is fully compatible, using the RF phase in HE linac, to also set the length of the single bunch needed for injection in the BR. Finally, Table 6 lists the relative cost of the different linacs in arbitrary units. In terms of cost and plug-power requirements, the HE linac is comparable to the other linacs and this basically means that, with this approach, the cost of the pre-injector linacs depends linearly on the beam energy to be achieved at the pre-injector end.

3 Positron Source: Target and Capture System (WP3)

Positron production is always an extremely important topic for any electron-positron collider. This is particularly true for future colliders such as FCC-ee, which are designed to operate at the extreme end of parameters, where a positron source with a high positron yield is required. Thus, the high-luminosity circular collider FCC-ee will need a low-emittance positron beam with high enough intensity to shorten the injection time. A positron bunch intensity of $2.5 \cdot 10^{10}$ particles is required at the injection into the collider rings. Positron rate foreseen at FCC-ee is within a factor of 2 compared to the positron rate obtained at the SLC at SLAC and is an order of magnitude lower than the typical values foreseen for the Linear Collider projects [5]. At the pre-injector level, the main specification for the positron source design is to provide the positron bunch charge of 5.4 nC accepted in the Damping Ring (DR), including the transmission efficiencies from the DR up to the collider ring. Based on the available experience of designing and operating previously or currently operated positron sources, a safety margin of 2.5 is now applied for the whole FCC-ee positron source studies. Thus, a total positron bunch

Table 5: RF power source parameters. The two options for the HE linac are both listed.

Linac	Freq.	Peak power specification	Rep. rate	RF pulse length	Duty factor	Average power	Required numbers
	[MHz]	[MW]	[Hz]	[μ s]	[10^{-3}]	[kW]	
p-linac	2004	80	200	5	1	80	16+1
e-linac	2806	80	200	3	0.6	48	10+1
c-linac	2806	50	400	3	1.2	60	35
HE linac	2806	80	200	3	0.6	48	82
HE linac	5611	50	200	3	0.6	30	86

Table 6: Relative cost of linacs in the pre-injector in arbitrary unit.

Linac	Klystron cost	HV Modulator cost	Cost estimation
p-linac	0.27	0.9	32.5
e-linac	0.18	0.82	20.5
c-linac	0.19	0.85	66.5
Total p-, e-, c-linac			119.5
HE linac - S-band option	0.18	0.82	152.5
HE linac - C-band option	0.16	0.80	155

intensity of 13.5 nC should be delivered to the DR.

Two methods are investigated for positron production for the FCC-ee to obtain the required performances. The first one is based on a conventional positron source using 6 GeV electrons impinging on a 17.5 mm thick tungsten target. The bremsstrahlung radiation of the electrons in the field of the nuclei is converted in e^+e^- pairs. This scheme has been used for all the e^+e^- colliders (ADA, ACO, DCI, SPEAR, ADONE, LEP, and also for the first linear collider SLC). The experience has been mainly successful. However, due to the high number of electrons in the short bunch of SLC, the breakdown analysis of the used target led to a limitation in the deposited power density expressed in J/g [17]. Its maximum value (PEDD), for tungsten targets, is about 35 J/g. Such limitation has some consequences on the incident electron beam size and the target thickness limitations. A second approach is based on the production of a large number of photons in thin crystal targets oriented on their main axes. Electrons propagating in the crystal at glancing angles to the axes are channeled and emit a large number of soft photons due to the collective action of a large number of nuclei [9]. Such method has been successfully tested at CERN and KEK [8, 3, 21, 19]. These investigations led to a concept of so-called hybrid positron source [22] associating a thin oriented crystal with an amorphous converter and a sweeping magnet in between to sweep off the charged particles emitted in the crystal, allowing only the photons to hit the amorphous converter [18]. This approach involving the sweeping magnet is of great importance especially for the linear colliders, where the drive beam power can reach very high values. Thus, for the FCC-ee positron source, two options (conventional and hybrid) were considered, but at this time the conventional production scheme is currently assumed for pre-injector design studies and cost estimation.

The capture section comprises an Adiabatic Matching Device (AMD) [7] followed by the capture linac embedded in a DC solenoid magnetic field to accelerate the beam until about a few hundreds of MeV positron beam energy. Currently, we have assumed a 200 MeV as the end of the capture linac and placement of the electron-positron separation section (chicane). Then, the solenoid focusing is employed until 735 MeV of positron beam energy but studies are ongoing to define the energy at which the positrons could pass to the quadrupole focusing and be further accelerated up to the 1.54 GeV (energy of the DR). For the capture linac, several types of the RF structures have been considered up to now and the final choice for the positron linac is a 3-meter-long, TW 2 GHz ($2a = 60$ mm) RF structures providing larger iris apertures, which results in the

larger transverse acceptance of the positrons. Two options are currently considered for the AMD: the first involves the use of a Flux Concentrator (FC), which makes use of a pulsed magnet, a technology presently used in the positron source of the SuperKEKB collider [23], while the second involves the use of a Superconducting solenoid (SC). The latter is based on the High-Temperature Superconducting (HTS) material with which the solenoid coils will be constructed. This technology will also be tested in the Swiss-FEL experiment at PSI [20]. Two models for FC were considered, the first was studied by BINP while the second is based on the current FC used in SuperKEKB. Due to the conceptual and mechanical constraints of the FC, the peak of the magnetic field is located downstream the target and as a result, the available field on the target is reduced to 3.5 T/ 1.1 T (for the BINP/SuperKEKB designs respectively) manifesting a significant drop in capture efficiency. Moreover, the presence of a high transverse magnetic field component (with strong domination of dipole harmonic) makes the trajectories of positrons strongly distorted. As a result, the positron beam receives an offset in vertical and horizontal planes. This eventually should be mitigated for the positron beam transport in the capture linac. Compared to SuperKEKB (or BINP) FC, higher repetition rate (up to 200 Hz–300 Hz) and ideally higher magnetic field value and aperture are requested for the future collider projects including FCC-ee. In this framework, one of the solution is to make use of the SuperKEKB experiences and join the effort on the FC design studies and prototyping between FCC/ILC/CLIC collaborations to arrive to a more realistic and reliable FC model.

In this framework, it was proposed to explore the use of an SC solenoid based on the HTS technology for positron capture. For the AMD based on the SC solenoids, the HTS field map is adopted from the P³ project [20]. The HTS solenoid used as the AMD provides much higher field value on the target exit surface, larger aperture and flexible target position as the target can be placed inside the magnet bore. Thanks to the axial symmetry of the solenoid, the transverse magnetic field at the magnet axis is equal to zero and, therefore, no beam distortion is expected compared to the FC option.

In summary, the current baseline for positron production, capture and linac includes the following components:

- Positron production: conventional scheme.
- Matching device is based on the SC solenoid (5 HTS coils, 72 mm bore aperture including shielding)
- Capture linac and positron linac are based on the large-aperture L-band TW RF structures (2 GHz, 3-m long accelerating structures)
- The positron and electron bunches are separated at the end of the capture system by a chicane at 200 MeV and the solenoid focusing is used until 735 MeV of positron beam energy
- NC solenoid with the field of $B = 0.5$ T (realistic field profile) is assumed for the capture linac and positron linac.

Table 7: Parameters and simulation results for the positron sources under study. For the matching device three options are considered, two with the flux concentrator (BINP FC and SuperKEKB FC) and one with the superconducting solenoid (HTS solenoid). CS: capture system, DR: damping ring.

Drive beam parameters	Alternative FC-based capture system		Capture system v1	Unit
	BINP FC	SKEKB FC	HTS solenoid	
Matching Device (MD)	8-44	7-52	72	mm
MD aperture	7.5 (3.5)	4.4 (1.1)	15 (12)	T
MD peak magnetic field (@Target)	3.1/7.4	5/12	2.1/5	nC/kW
e-beam bunch charge/e-beam power	1.7/11.1	2.9/18.3	1.2/3.1	kW/(J/g)
Target deposited power/PEDD	4.9	3.3	8	N_{e^+}/N_{e^-}
Positron yield @CS	4.4	2.7	6.5	N_{e^+}/N_{e^-}
Positron yield @DR	12.2	11.9	13.7	mm.mrad
Normalized emittance (rms)	1.2	1.1	1.4	%
Energy spread (rms)	2.9	2.6	2.9	mm
Bunch length (rms)	13.5			nC
e+ beam bunch charge				

Tab. 7 summarizes the main results of the positron production and capture simulations for both, FC- and HTS solenoid-based capture systems. At this stage, an energy-longitudinal position cut around the highest density of positrons made within the DR acceptance allows defining the accepted positron yield¹. Later on, the positron tracking simulations in the positron linac followed by the injection in the DR should be carried out to have more realistic estimate of the accepted positron yield. However, beam dynamics simulations have shown that both schemes can guarantee positron production even with some safety margin.

Until now, studies of radiation load and target design have focused exclusively on the SC solenoid approach. The results obtained so far have shown no showstoppers in using HTS technology for the matching device. The integration of the target is being studied and will be experimentally verified in the P³ experiment.

4 Damping Ring and Transfer Lines (WP4)

The purpose of the Damping Ring (DR) design is to accept the 1.54 GeV beam coming from the positron linac, damp the positron(/electron) beams, and provide the required beam characteristics for injection into the common linac (see Fig. 1). In this regard, the DR has quite challenging design requirements. DR should reduce by orders of magnitude the beam emittance in particular for the positron beams, and should provide large beam acceptance in order to catch the beam from the positron linac, which has a large distribution in the 6D phase space. A complex system of Transfer Lines includ-

¹For the results presented in Tab. 7 the energy window cut of $\pm 3.8\%$ and longitudinal position window of 16.7 mm (or 40 degrees in terms of the phase) have been used.

ing doglegs to implement injection and extraction in and from the DR, and arcs brings back the cooled positron beam to the entrance of the common linac stage. An Energy Compressor (EC) System installed between the positron linac and the DR is used to reduce the incoming beam energy spread in order to maximize the injection efficiency. A bunch compressor at the entrance of the common linac is used to keep under control the rms bunch length of the incoming positron beam. The repetition rate of common linac is 400 Hz with two bunches per RF pulse. This configuration imposed to revise the Damping Ring injection-extraction timing in order to account for the additional time necessary to avoid the presence of two different kinds of particles in the same common linac RF pulse.

The DR is about 240 m long and the energy is selected to avoid spin resonances. According to the current design, a FODO-type cell is chosen, the DR is made up of two arcs and two straight sections housing the damping wiggler magnets, RF cavity, and injection/extraction equipment. The injection will be done by using an on-axis scheme. The DR beam structure foreseen a sequence of a maximum of 9 bunch trains, each of them including two bunches. Single bunch current is planned to reach a rather high intensity as it varies in the range of 0.6÷5.7 mA. The injected beam must reach the nominal equilibrium emittance of 0.96 nm in a store time of about 40 msec. High currents stored in rather short bunches, require a careful evaluation of beam lifetime and a comprehensive analysis of collective effects taking into account a realistic impedance budget, and considering beam coupling with the RF system. Preliminary analytical estimations [15] of various collective effects such as space charge (SC), intra-beam scattering (IBS), longitudinal micro-wave instability, transverse mode coupling instability (TMCI), ion effects, electron cloud and coherent synchrotron radiation (CSR), have been performed for an intermediate version of the DR optics. No major limitations are expected from IBS, TMCI and CSR. Concerning the SC, the tune shift at the equilibrium state might be an issue. Furthermore, the Boussard criterion is below the longitudinal impedance assuming a vacuum chamber radius of 10 mm. It was shown that the neutralization density exceeds the e-cloud instability threshold for the equilibrium state. The fast rise times of the fast ion instability can be compensated with a feedback system, provided a vacuum pressure of 10^{-9} mbar is achieved in the DR. The straight sections are designed to host four wigglers, two RF cavities and the Injection/Extraction equipment. Table 8 lists the main parameters of the the DR.

In the following considerations on the DR longitudinal dynamics we assume to use as RF cavity the LHC type SC device operating at the frequency of 400 MHz, as already proposed in the CDR [4]. This cavity consists of two RF modules housed in the same cryostat. It is worth reminding, that in the following we will indicate as RF voltage the total voltage of the two RF modules. In Tab.9 is reported a summary of the beam dynamics parameters computed for several RF voltages and considering momentum compaction, $\alpha_c = 0.001535$, harmonic number, $h = 319$, and a total length, $L = 239.2629$ m. The listed parameters are calculated for stationary bunches at the equilibrium, and in the zero-current approximation. In order to get more realistic quantities, it is necessary to perform comprehensive numerical simulations taking into account the number of circulating particles, the ring impedance, how the beam couple with the ring impedance,

Table 8: Damping Ring parameters (as in CDR [1]).

Parameters		Unit
Circumference	241.8	m
Equilibrium emittance (x/y/z)	0.96/-/1.46	nm/nm/um
Dipole length, field	0.21/0.66	m/T
Wiggler #, length, field	4, 6.64, 1.8	-/m/T
Cavity #, length, voltage	2, 1.5, 4	-/m/MV
Bunch # stored, charge	16, 3.5	-/nC
Damping time $\tau_x/\tau_y/\tau_z$	10.5/10.9/5.5	ms
Store time	40	ms
Kicker rise time @1.54GeV	50	ns
Energy loss per turn	0.225	MV
SR power loss wiggler	15.7	kW

RF beam loading, and RF transient beam loading. In the present DR configuration high RF voltage determines rather short bunch length values, which can represent an issue for beam lifetime and for several collective effects. This aspect together with the result obtained from tracking studies about transverse beam acceptance led us to fix $V_{RF} = 4$ MV as a baseline for the RF cavity voltage.

The Dynamic Aperture (DA) has been evaluated using the PTC [16] module of MAD-

Table 9: Longitudinal beam dynamics parameters. In bold the parameters for the baseline of the RF system.

Parameters					Unit
$\Delta E/E_s$	0.71×10^{-3}				
T_0	0.79801				μs
ω_0	7.87×10^6				$s^{-1}rad$
V_{RF}	8 MV	6 MV	4 MV	2 MV	MV
Ω_S	25.13	21.918	17.888	12.618	kHz
ν_s	0.003215	0.00278	0.002272	0.0016	
Bunch length (rms)	2.07	2.39	2.93	4.15	mm
ϕ_S	0.0283967	0.0378663	0.0568164	0.113817	rad
$E - E_S$	0.124	0.107	0.0862	0.058	GeV
$\Delta\phi$	1.8	1.7769	1.7269	1.6016	unit of π
L_{bucket}	0.6788	0.6664	0.6476	0.6006	m

X [13] using two different approaches:

quick: the tracking has been performed starting in the transverse plane on a random position within a box of 4×4 cm². The particles have been tracked up the 2000 turns without radiation damping. The initial energy deviation has been considered up to 5%. In Fig. 4-left the result of this tracking is shown. At the nominal energy in both planes, the stable region, normalized as a function of beam width, is of the order of three $\sigma_{h,v} = \sqrt{\beta_{h,v}\epsilon_{h,v} + (D_{h,v}\delta_E)^2} \simeq 3mm$.

full: tracking performed using the CDR [1] nominal 6D beam envelope at the injection

with radiation damping enabled. Positrons have been tracked for 10000 turns, corresponding to a store time equal to the damping time in the DR. The injected beam emittance in the transverse planes is assumed to have the CDR nominal parameters: $\epsilon_{h,v}^{geo} = 1.29, 1.22$ mm mrad, , respectively for horizontal and vertical and $\delta_E \simeq 5\%$ for the energy spread. The result is shown in Fig. 4-right.

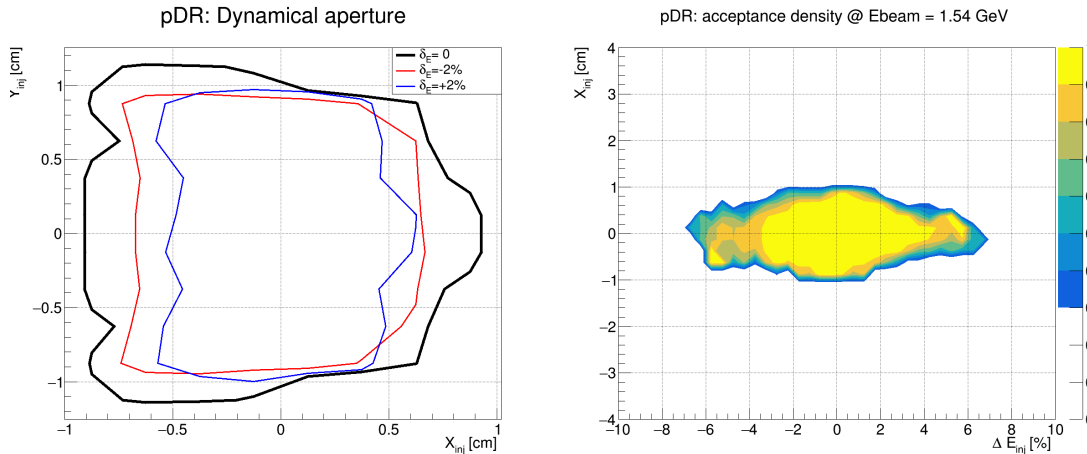


Figure 4: Dynamic aperture. In the left plot, the transverse stable region is shown for the nominal beam energy (1.54 GeV - black) and for $\pm 2\%$ energy relative deviation (blue and red, respectively). While the stable region is kept quite constant within 2% energy spread is observed to drop significantly for higher deviations. In the right plot, the result of the *full* simulation is reported. The color map represents the fraction of survived particles at the end of the tracking as a function of the initial horizontal position and energy deviation. The survival probability includes the full 6D particle phase space treatment. The beam is assumed to be Gaussian distributed with CDR nominal widths in the transverse plane.

With the current DR lattice and the CDR [1] incoming beam parameters, the DR acceptance is estimated to be $\epsilon_{ACC} \simeq 47\%$ thus implying a factor of two of reduction in the positron yield. The DA estimation shows that the DR acceptance is greatly reduced when the relative energy spread of the incoming positron beam exceeds 2%. To overcome this limitation, the energy distribution can be compressed using an energy compressor (ECS) located downstream of the positron linac [2], as shown schematically in Fig. 1. The effect of the ECS on the incoming beam is a reduction of the total energy spread and a corresponding increase in the bunch length. One possible option for the ECS is to use four curved rectangular dipoles in the so-called C-channel, followed by an additional RF module like the one used in the positron linac. In such a magnetic chicane the first- and second-order dispersion are intrinsically closed without using quadrupoles. Using the ECS reduces the energy spread thus increasing the number of positrons accepted by

the DR. Tracking simulations were carried out using the particle distributions from the positron linac end passing through the ECS and considering 10000 turns in the DR. The simulation results showed an overall positron acceptance in the DR of about 86%. An important aspect to note is that start-to-end tracking simulations were performed, from the target to the injection into the DR. This aspect will be important to optimise the entire positron production chain by finding the right compromise between emittance, energy spread and positron yield.

Regarding to the injection and extraction timing, the positron bunches (two per RF pulse) are produced at the positron source synchronized with the electron bunches timing while the extracted ones from the DR have to be synchronized with the positron accelerating RF pulses of the common linac. This requirement together with the cooling time needed to reach the proper beam parameters (emittance) at the extraction fully defines the timing scheme of the DR. To reach the target values of the emittance at the extraction a minimum stored time of 40 ms is needed (four damping times), while to shift from the time series of the electron pulses to the one for the positrons in the common linac, an additional store time of 2.5 ms is required. Such a delay can be accommodated only if a minimum number of nine linac pulses are stored in the DR. The timing of the primary electron pulses has to be properly scaled according to the following relation:

$$T_{gun}(i) = iT_{Rep} + \Delta_b T_{RF}(i\%N_p) \quad i \in [0, n] \quad (1)$$

where T_{Rep} is the period of the injection pulse rate (200 Hz), Δ_b is the time differences between the first filled buckets in the DR for each pulse², T_{RF} is the radio-frequency of the DR (400 MHz) and N_p is the number of stored pulses in the DR (9 minimum). As shown in the Eq. 1, the effective time of the electron pulses has to be adjusted within the range of the revolution period ($T_S \approx 1\mu s$). Analogously the extraction time has to follow this relation:

$$T_{Ext}(i) = T_{gun}(i) + \Delta T_{DR} + T_S/2 + T_{Rep}/2 - \Delta T_{12} \quad (2)$$

where ΔT_{DR} is the minimum store time, $T_S/2$ takes into account the DR half turn between the injection and extraction section, $T_{Rep}/2$ takes into account the extra time to slide from electron to positron common linac timing and ΔT_{12} represent a fixed phase adjustment that takes into account the propagation time from DR to the entrance in the common linac. The Eq. 2 shows that it is possible to adjust the extraction timing only in units of the revolution period.

The design of the Transfer Lines (TLs) is inspired by criteria of high modularity, suitable to deal with a project in constant evolution, and, as a consequence, requiring frequent modifications. The TLs include a line driving the positron beam from the linac to the DR injection section ($pTLi$), and an extraction line bringing the cooled beam back to the common linac ($pTLe$). The $pTLe$ is based on a combination of periodical straight section

²Since linac pulses contain two bunches, the effective time structure of filled buckets in the DR depends not only by the number of stored pulses but also from the arrival time difference between the two bunch in the same pulse. Currently, this time difference is set at 25 ns because of the main ring requirements.

modules, implemented by a FODO magnetic structure, and arcs built by combining basic cells providing 30 degrees of deflection each. The arcs in the *pTLe* are periodic structures based on isomagnetic triple bend cells (TBA). The bends are rectangular magnets providing 10 degrees deflection angle each, but having asymmetric lengths, with the central being the shorter one. Each cell is achromat, isochronous, has moderate betatron oscillation amplitude both in the horizontal and in the vertical plane, and moderate maximum horizontal dispersion excursion, $|\eta_x| < 0.3$ m. The cell also features very low \mathcal{H} function values suitable to avoid possible beam quality degradation induced by CSR emission.

The design of the bunch compressor needed to reduce the length of the bunch before

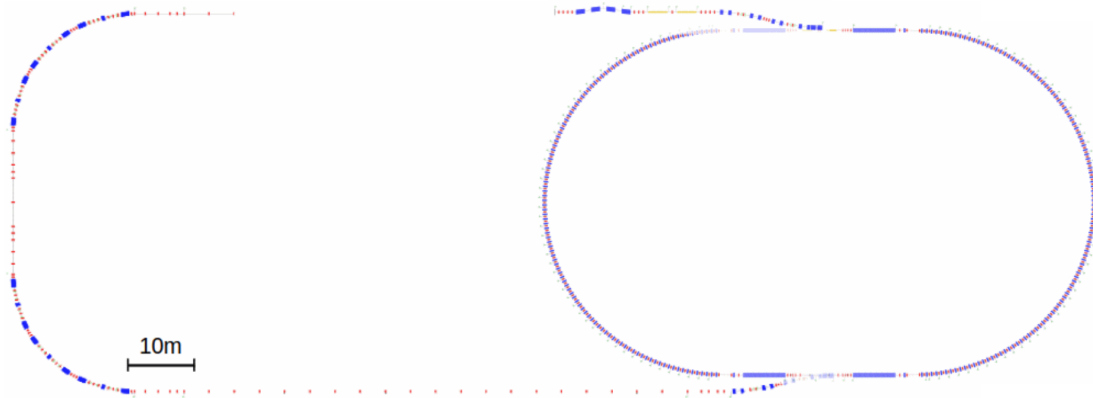


Figure 5: Overall layout of the transfer lines, ECS and DR.

injection into the common linac was also finalised. It includes a magnetic chicane and two RF modules like those used in the common linac. For cost estimation, a table was prepared with a breakdown of the components used for the different parts from the positron linac end to the entrance of the common linac, overall layout is shown in Fig. 5.

5 PSI Positron Production (P^3) Project (WP6)

The P^3 experiment [20] is a demonstrator for the positron source described in chapter 3. More details of the experiments can be found here [14]. The goal is to design and install such demonstrator in the SwissFEL facility, and validate through an experiment a range of novel techniques that, according to simulations, have proven potential to increase the e^+ yield by one order of magnitude with respect to the state of the art. The experiment layout is shown in Fig. 6, featuring a e^+ source based on a 6 GeV electron beam and 17.5 mm-thick (or 5 times the radiation length) amorphous Tungsten target, followed by a capture system consisting of a high-field solenoid system and 2 RF accelerating cavities. The remarkable e^+ capture capabilities of P^3 are enabled to great extent by the usage of high temperature superconducting (HTS) solenoid around the target region, as well as a novel standing wave solution for the RF cavities that provides a large iris aperture (see Table 10). In addition, the experiment diagnostics, whose goal is to demonstrate such a

e^+ yield upgrade, consisting of an arrangement of broadband pick-ups, 2 Faraday cups and a variety of scintillating screens and fibers. This setup will detect simultaneously the e^+e^- bunching structure after the RF cavities, and measure the bunch charge and energy spectrum of e^+ and e^- streams separately.

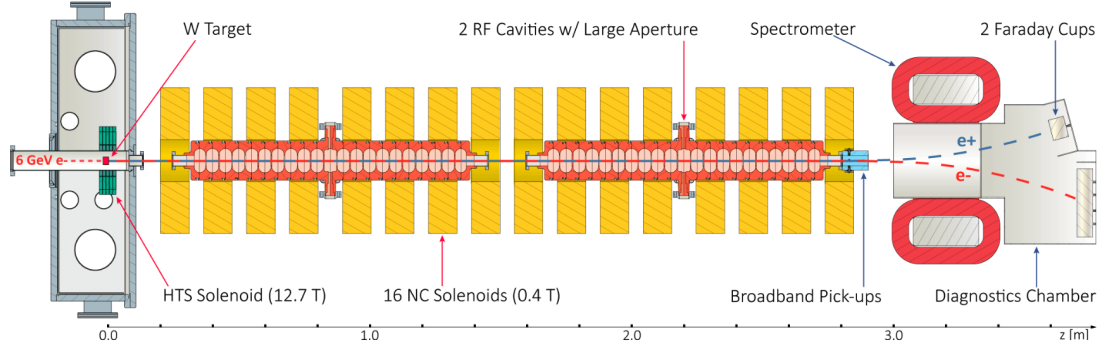


Figure 6: Layout of the P3 experiment featuring key hardware components (red arrows) and diagnostics (blue arrows).

The P³ project is driven by the luminosity requirements of the future supercollider FCC-ee [1], and its results will constitute one of the main deliverables of the FCC-ee injector feasibility study [10]. Although the experiment is designed to reproduce the beam dynamics of the FCC-ee e^+ source [6], the primary e^- beam current parameters were decreased in order to meet the SwissFEL radiation protection limits. Notice in

Table. 10 the differences in bunch charge, repetition rate and the number of bunches per pulse with respect to the FCC-ee baseline.

Table 10: Main e^+ source parameters of FCC-ee and P^3 .

	FCC-ee	P^3
Energy [GeV]	6	
Max. sol. field at Target [T]	tbd	12.7
Avg. sol. field along linac [T]	0.5	0.45
Min. RF cavity aperture [mm]	60	40
σ_E	0.1%	
σ_t [ps]	3.33	
σ_x, σ_y [mm]	0.5	
σ_{px}, σ_{py} [MeV/c]	0.06	
Target length [mm]	17.5	
Q_{bunch} [nC]	1.7 - 2.4	0.20
Repetition rate [Hz]	200	1
Bunches per pulse	2	1

The SwissFEL facility is an ideal host for the P^3 experiment since it can provide a 6 GeV electron beam, corresponding to the nominal drive beam energy of the FCC-ee positron source (see Table 10). Two beam lines (Aramis and Athos) are currently operating at SwissFEL, while the accelerator tunnel already foresees space for a future, third beam line (Porthos) leaving enough room for the installation of the P^3 bunker and switchyard. Fig. 7 shows the current, and almost final, design version of the P^3 experiment. According to the preliminary timeline, the currently ongoing works are expected to conclude by the end of 2025, as operation with e^+ is envisaged for 2026.

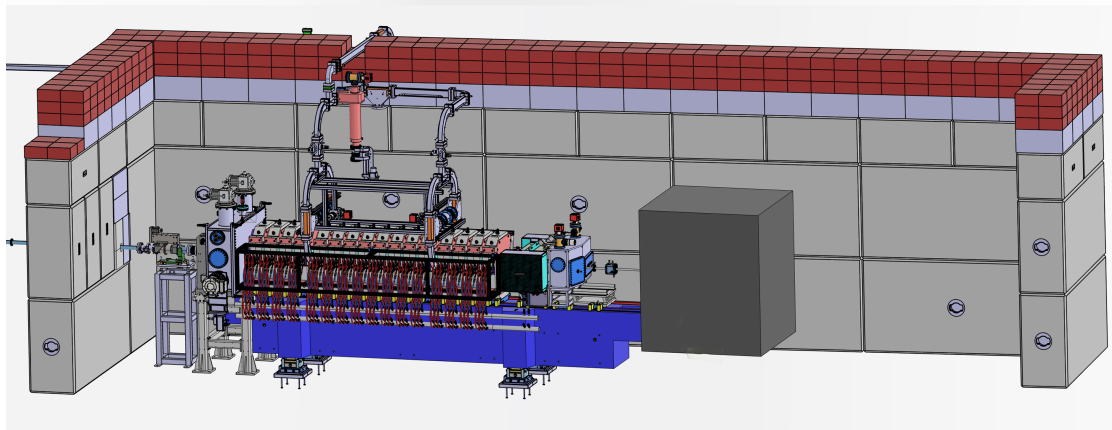


Figure 7: View of the P^3 experiment in its bunker. Including rough model of the beam dump.

References

- [1] A. Abada et al. FCC-ee: The Lepton Collider. *Eur. Phys. J. ST*, 228(2):261–623, 2019.
- [2] K. Akai, K. Furukawa, and H. Koiso. Superkekb collider. *Nuclear Instruments and Methods in Physics Research Section A: Accelerators, Spectrometers, Detectors and Associated Equipment*, 907:188–199, 2018.
- [3] X. Artru. Summary of experimental studies, at cern, on a positron source using crystal effects. *Nuclear Instruments and Methods in Physics Research Section B: Beam Interactions with Materials and Atoms*, 240:762–776, 2005.
- [4] D. Boussard and T. Linnecar. The lhc superconducting rf system. Technical report, CERN, 1999.
- [5] I. Chaikovska, R. Chehab, V. Kubytskyi, S. Ogur, A. Ushakov, A. Variola, P. Sievers, P. Musumeci, L. Bandiera, Y. Enomoto, M.J. Hogan, and P. Martyshkin. Positron sources: from conventional to advanced accelerator concepts-based colliders. *Journal of Instrumentation*, 17(05):P05015, may 2022.
- [6] I. Chaikovska et al. Positron Source for FCC-ee. In *Proc. 10th International Particle Accelerator Conference (IPAC'19), Melbourne, Australia, 19-24 May 2019*, number 10 in International Particle Accelerator Conference, pages 424–427, Geneva, Switzerland, Jun. 2019. JACoW Publishing. <https://doi.org/10.18429/JACoW-IPAC2019-MOPMP003>.
- [7] R. Chehab. Positron sources. Technical report, 1992.
- [8] R Chehab, R Cizeron, C Sylvia, V Baier, K Beloborodov, A Bukin, S Burdin, T Dimova, A Drozdetsky, V Druzhinin, M Dubrovin, V Golubev, S Serednyakov, V Shary, V Strakhovenko, X Artru, M Chevallier, D Dauvergne, R Kirsch, Ph Lattes, J.-C Poizat, J Remillieux, A Jecic, P Keppler, J Major, L Gatignon, G Bocek, V Kulibaba, N Maslov, A Bogdanov, A Potylitsin, and I Vnukov. Experimental study of a crystal positron source. *Physics Letters B*, 525(1):41–48, 2002.
- [9] R. Chehab, F. Couchot, A. R. Nyaiesh, and F. Richard and X. Artru. Study of a positron source generated by photons from ultrarelativistic channeled particles. In *Proc. 13th Particle Accelerator Conference, PAC'89 - 13th Particle Accelerator Conference*, pages 283–285, 1989.
- [10] P. Craievich et al. The FCCee Pre-Injector Complex. In *Proc. IPAC'22*, number 13 in International Particle Accelerator Conference, pages 2007–2010. JACoW Publishing, Geneva, Switzerland, 07 2022.

- [11] P. Craievich, M. Schaer, N. Vallis, and R. Zennaro. Fcc-ee injector study and p³ project at psi, chart scientific report 2021. Technical report, CHART (Swiss Accelerator Research and Technology), 2022.
- [12] P. Craievich, B. Simona, Jean-Yves Raguin, Mattia Schaer, Nicolas Vallis, Riccardo Zennaro, Steffen Doebert, Jean-Louis Grenard, Alexej Grudiev, Barbara Humann, Andrea Latina, Anton Lechner, Ramiro Mena Andrade, Antonio Perillo-Marcone, Yongke Zhao, Zdenek Vostrel, Fahad Alharthi, Iryna Chaikovska, Viktor Mytrochenko, Antonio De Santis, and Catia Milardi. FCC-ee Injector Study and P³ Project at PSI, CHART Scientific Report 2022. Technical report, CHART (Swiss Accelerator Research and Technology), 2023.
- [13] L. Deniau, H. Grote, G. Roy, and F. Schmidt. The mad-x program: User’s reference manual (v.5.08.01). Technical report, CERN, 2022.
- [14] N. Vallis et al. Proof-of-principle e+ source for future colliders. *Phys. Rev. ST Accel. Beams*, 27:013401, 2024.
- [15] O. Etisken, F. Antoniou, A. De Santis, C. Milardi, and F. Zimmermann. Collective effects estimates for the damping ring design of the fcc-ee. In *Proceedings of the 13th International Particle Accelerator Conference, IPAC’22 - 13th International Particle Accelerator Conference*, pages 2435–2438, 2022.
- [16] E. Forest, F. Schmindt, and E. McIntosh. Introduction to the polymorphic tracking code. Technical report, 2002.
- [17] J. Sheppard. Conventional positron target for a tesla formatted beam. Technical report, SLAC, 2003.
- [18] L. Bandiera *et al.* Crystal-based pair production for a lepton collider positron source. *The European Physical Journal C*, 82:699, 2022.
- [19] M. Satoh *et al.* Experimental study of positron production from silicon and diamond crystals by 8-gev channeling electrons. *Nuclear Instruments and Methods in Physics Research Section B: Beam Interactions with Materials and Atoms*, 227:3–10, 2005.
- [20] N. Vallis *et al.* The psi positron production project. In *Proceedings of the 31st International Linear Accelerator Conference, Linac’22 - 31st International Linear Accelerator Conference*, pages 577–580, 2021.
- [21] T. Suwada *et al.* Measurement of positron production efficiency from a tungsten monocrystalline target using 4-and 8-gev electrons. *Phys Rev E Stat Nonlin Soft Matter Phys.*, 67:016502, 2003.
- [22] X. Artru *et al.* Polarized and unpolarized positron sources for electron–positron colliders. *Nuclear Instruments and Methods in Physics Research Section B: Beam Interactions with Materials and Atoms*, 266:3868–3875, 2008.

- [23] Y. Enomoto *et al.* A new flux concentrator made of Cu alloy for the SuperKEKB positron source. In *Proceedings of the 12th International Particle Accelerator Conference, PAC'89 - 13th Particle Accelerator Conference*, pages 2954–2956, 2021.

Publications and Conference Contributions

- FCC-ee Injector Studies Mini-Workshop, Apr 20-21, 2023, INFN Frascati National Laboratories, <https://agenda.infn.it/event/34369/>
- IPAC 2023 (7-12 May, Venice, Italy): <https://www.ipac23.org/>
 - N. Vallis et al., A positron source demonstrator for future colliders, <https://accelconf.web.cern.ch/ipac2023/doi/jacow-ipac2023-tupa086/>
 - V. Mytrochenko et al., On positron beam dynamics an initial part of a large aperture FCC-ee capture linac, <https://accelconf.web.cern.ch/ipac2023/doi/jacow-ipac2023-mop1086/>
 - F. Alharthi et al, Benchmarking the FCC-ee positron source simulation tools using the SuperKEKB results, <https://accelconf.web.cern.ch/ipac2023/doi/jacow-ipac2023-mop1094/>
 - I. Chaikovska et al, Update on the FCC-ee positron source design studies, <https://accelconf.web.cern.ch/ipac2023/doi/jacow-ipac2023-mop1095/>
 - Y. Zhao et al., Use of a superconducting solenoid as a matching device for the compact linear collider positron source, <https://accelconf.web.cern.ch/ipac2023/doi/jacow-ipac2023-mop1096/>
 - S. Spampinati et al., Damping ring and transfer lines of FCC-ee injector complex, <https://accelconf.web.cern.ch/ipac2023/doi/jacow-ipac2023-mopa112/>
 - O. Etisken et al., Considerations for a new damping ring design of the FCC-ee pre-injector complex, <https://accelconf.web.cern.ch/ipac2023/doi/jacow-ipac2023-mop1175/>
- FCC-ee week 2023 (5–9 Jun 2023, Millennium Gloucester Hotel London Kensington: <https://indico.cern.ch/event/1202105/>
 - Full-energy booster, A. Chance (CEA)
 - Pre-injector baseline and options, P. Craievich (PSI)
 - Positron production, capture and acceleration until the damping ring, I. Chaikovska (CNRS/IJCLab)
 - Design of the FCC-ee positron source target: current status and challenges, R. F. Mena Andrade (CERN)
 - Damping ring and transfer lines for the FCC-ee pre-injector complex, C. Milardi (INFN-LNF)
 - Linac beam dynamics, S. Bettoni (PSI)
 - Layout and design of positron and electron linacs up to 20 GeV, A. Grudiev (CERN)
 - SPS pre-booster option, H. Bartosik (CERN)
 - Siting and transfer lines, W. Bartmann (CERN)

- N. Vallis et al., *Proof-of-principle e^+ source for future colliders*, Phys. Rev. Accel. Beams 27, 013401 (2024), <https://journals.aps.org/prab/abstract/10.1103/PhysRevAccelBeams.27.013401>
- S. Doebert and Z. Vostrel, Design of an electron source for the FCC-ee with top-up injection capability, to be submitted to PR AB (2024).